Journal of
Ceramic Science
and Technology

J. Ceram. Sci. Tech., 07 [04] 429-432 (2016)
DOI: 10.4416/JCST2016-00067
available online at: http://www.ceramic-science.com

Fabrication of Tin-Doped Indium Oxide Thin Films Using Aerosol Deposition

Y. Hasegawa*, Y. Sato, S. Yoshikado

Graduate School of Science and Engineering, Doshisha University
received September 6, 2016; received in revised form October 25, 2016; accepted November 4, 2016

Abstract

Tin-doped indium oxide (ITO) thin films are a key material for optical devices owing to their high electrical conductivity and high optical transparency. In this study, ITO thin films were formed on glass and sapphire substrates at room temperature using aerosol deposition (AD), and their crystal structure, resistivity, and optical properties were investigated. The films maintained the crystal structure of the source ITO particles used to form the films. For the glass substrate, the resistivity of the ITO films was approximately 3.0×10^{-3} Ω·cm. In addition, when the thickness was 0.24 μm, the film exhibited high optical transmittance of approximately 90 % in the visible light region, which is higher than that of commercially available ITO thin film. The results show that AD can be used to fabricate ITO films with low resistivity and high optical transmittance.

Keywords: Tin-doped indium oxide, thin film, aerosol deposition, room-temperature impact consolidation, resistivity

I. Introduction

Transparent conductive films have recently become key components in various devices such as flat-panel displays and solar battery electrodes. Tin-doped indium oxide (ITO) is commonly used as the film material owing to its low resistivity and high optical transparency. ITO films are typically formed using sputtering deposition. Aerosol-assisted chemical transport (AACT) for the deposition of ITO thin films has also been reported [1]. However, unlike sputtering deposition, AACT is not a dry process. Therefore, sputtering deposition is applicable to various types of ceramic substrates owing to the strong adhesion to the substrate, the ability to modify films while maintaining the composition ratio of the target, and the ease with which the film thickness can be controlled. However, sputtering deposition is not suitable for the fabrication of thick films because of the low deposition rate. Furthermore, sputtering deposition requires heating of the substrate to obtain an ITO thin film with low resistivity. Therefore, ITO thin films cannot be fabricated on substrates with a low melting point, such as resins, using this method. In contrast, aerosol deposition (AD) is a novel technique that can be used to fabricate ceramic films at room temperature [2–11]. This technique is different from aerosol-assisted chemical vapor deposition or AACT because the source particles are deposited directly through a mechanism called room-temperature impact consolidation (RTIC), which is a dry process [2,3]. We previously reported that AD can be used to deposit thin films of titanium dioxide on various substrates, such as ceramics and resins, with a thickness that can be easily controlled via the gas flow rate and deposition time [5]. The films exhibited high densities, good adhesion to various substrates, and could be deposited over a large area under a low vacuum of several Pa. Furthermore, the fabricated films maintained the same crystal structure as that of the source materials. In this study, we evaluate the properties of ITO thin films formed using AD.

* Corresponding author: dup0307@mail4.doshisha.ac.jp

II. Experimental

Fig. 1 shows a schematic diagram of the AD apparatus [5], which consists of a deposition chamber and an aerosol chamber connected in series by transportation tubes. The deposition chamber is used for depositing ceramic films. It has a fixed narrow slit nozzle (5 mm × 0.3 mm), a substrate holder mounted on a motorized XY translation stage, and a heating system for the substrate. Before film formation, both the deposition chamber and the aerosol chamber are evacuated to approximately 2 Pa by means of a mechanical booster pump and an oil-sealed rotary pump. The ITO particles, which have an average diameter of approximately 700 nm, were dried by heating at 200 °C for 2 h under vacuum to prevent agglomeration.

The dried ITO particles were mixed with soda-lime glass beads (average diameter 1 μm) and supplied into the aerosol chamber. The glass beads were used to facilitate dispersion of the ITO particles in the aerosol chamber. The mixture of dried ITO particles and glass beads was mixed with a nitrogen carrier gas (N_2) to generate a colloidal aerosol in the aerosol chamber. In addition, the aerosol chamber was continuously vibrated to create a fine colloidal aerosol. The carrier gas flow was controlled with a mass flow controller. Only the ITO aerosol was transported by the carrier gas from the aerosol chamber to the deposition chamber using the pressure difference between the two chambers, while the glass beads remained in the aerosol chamber. The ITO particles were accelerated to

the speed of sound through the nozzle and were ejected toward the substrate. The distance from the nozzle to the substrate was fixed to 10 mm. The ITO particles were pulverized by collisions with the substrate and the already deposited film.

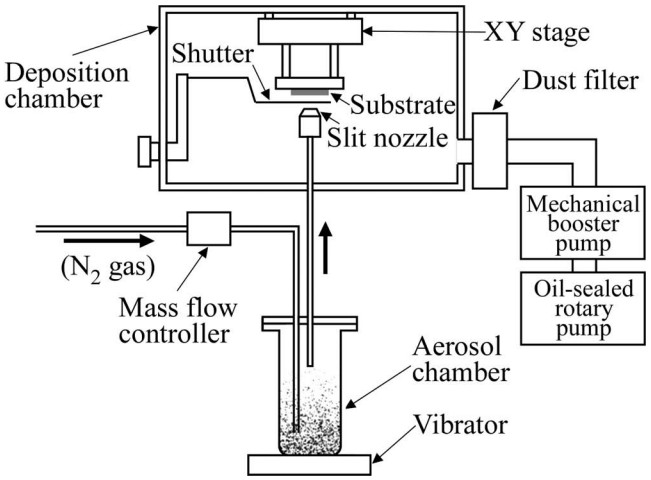

Fig. 1: Schematic diagram of the AD equipment.

Glass or a wafer of optically polished single-crystalline sapphire (c-axis) was used as the substrate. The substrate was placed on an XY stage, which was scanned at 100 μm/s to deposit a film of uniform thickness. The substrate temperature was varied from room temperature to 300 °C. The surface of the film was observed using a scanning electron microscope (SEM; JSM7500FA, JEOL). The thickness of the films was measured using a profilometer (DEKTAK150, Veeco). The crystal structure was analyzed using x-ray diffraction (XRD; Cu $K\alpha_1$, X'Pert, Panalytical). The resistivity of the film was measured using the four-probe method at room temperature, and the optical transmittance was measured using a visible-light spectrometer (U-3900, Hitachi).

III. Results and Discussions

A highly transparent film was deposited using a carrier gas flow rate of 2 – 8 L/min. The film did not separate from the substrate, even under ultrasonication in water, so it was concluded to be strongly adhered to the substrate. Fig. 2 shows SEM images of the surface of the films deposited on the glass and sapphire substrates. The average diameter of the ITO particles used to form the films was approximately 700 nm, while the size of the ITO grains in the films ranged from several tens of nm to 200 nm. This indicates that the ITO particles were pulverized by collisions with the substrate or the already deposited film. Fig. 3 shows XRD patterns for the ITO particles and the films deposited on the sapphire and glass substrates at room temperature. In_2O_3 has three crystalline phases, the two most common being the cubic ($I2_13$) and hexagonal (Rc) phases. The crystal structure of ITO is almost the same as that of cubic In_2O_3. Because the diffraction angles for the films were almost the same as those for the ITO particles, except for unidentified diffraction peaks that appeared for the film deposited on glass, the film was confirmed to be ITO. Based on the XRD spectra, the deposited film maintained the same crystal structure as that of the source ITO particles. Owing to the decrease in the ITO grain size in the film [5], the diffraction peaks for the ITO thin film were broad and the intensities were weak compared with those of the source particles. In contrast, the unidentified diffraction peaks were sharp. Using the Scherrer equation, the ITO grain size in the films was estimated to be approximately 20 nm for the films deposited on both types of substrate from the full width at half maximum (FWHM) of a diffraction peak [12]. However, the actual grain size of the ITO is larger than 20 nm because the Scherrer equation provides an overestimation; this is confirmed by the SEM images shown in Fig. 2. For all the films deposited at room temperature, a marked preferred orientation of the ITO grains was not observed.

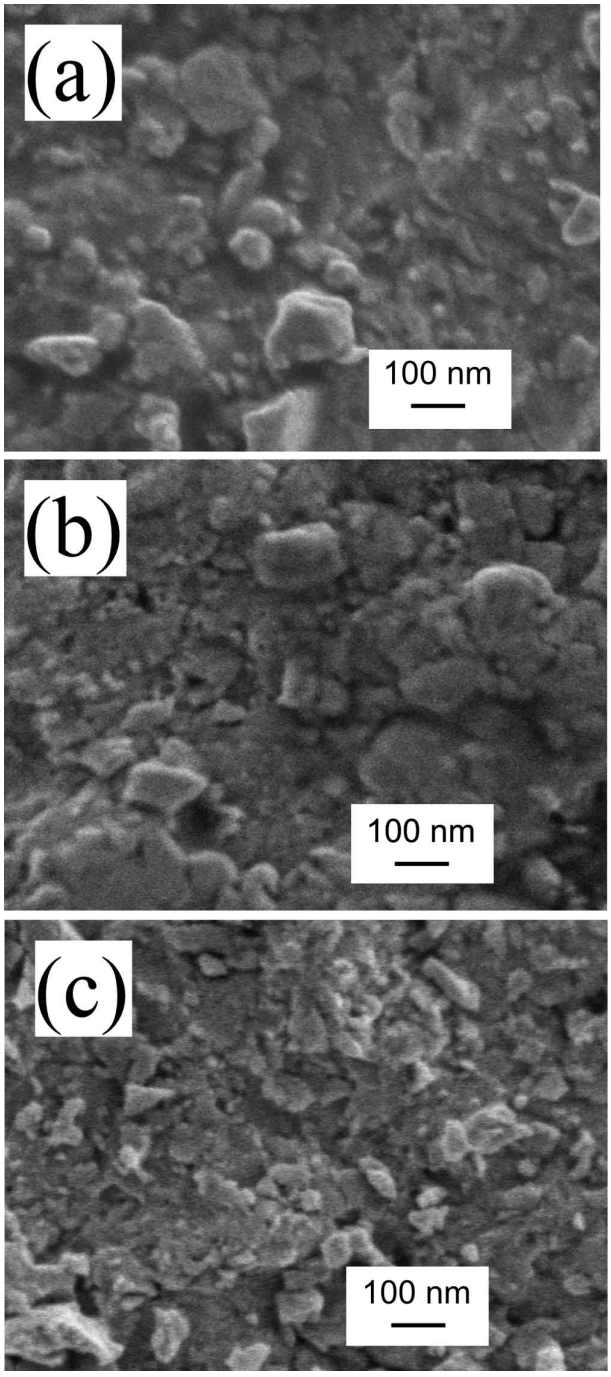

Fig. 2: SEM images of surface of film deposited on glass substrate at room temperature (a) and at 300 °C (b), and on sapphire substrate at RT (c).

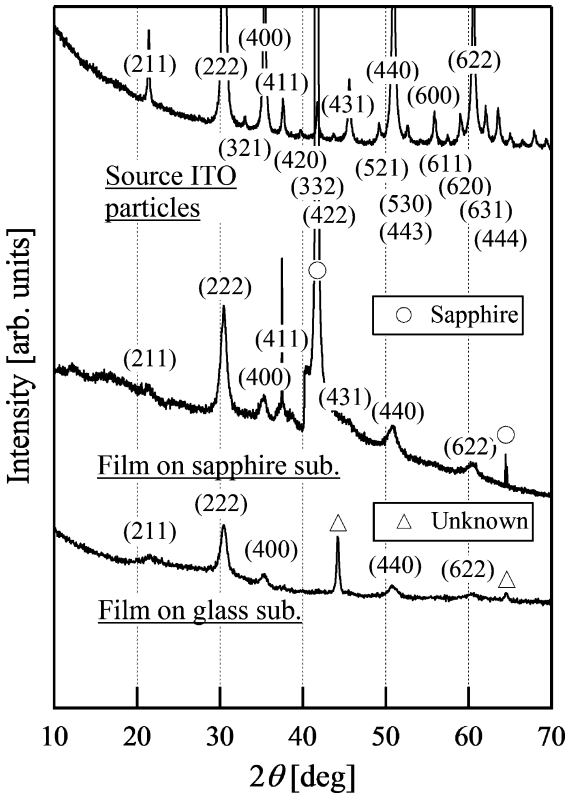

Fig. 3: XRD patterns of raw particles and films deposited on sapphire and glass substrates. Miller indexes correspond to ITO.

Fig. 4 shows the dependence of both the film thickness and the resistivity on the gas flow rate at room temperature. With a carrier gas flow rate of 2 L/min and a scan number of 10, the thickness was approximately 0.7 μm. The thickness increased linearly with increasing carrier gas flow rate. The resistivity was approximately $3-7 \times 10^{-3}$ Ω·cm and was larger than that of commercially available ITO thin film, as indicated by the dashed line in the figure, by a factor of 20 or more. Fig. 5 shows the dependence of the resistivity on the substrate temperature for a film deposited on a glass substrate. The carrier gas flow rate was 4 L/min and the number of scans was 10. The resistivity was approximately $3.8-9.7 \times 10^{-3}$ Ω·cm over the range of substrate temperatures studied. In contrast, the resistivity for the film deposited on the sapphire substrate shown in Fig. 2(c) was larger at 1.5×10^{-2} Ω·cm, even though the ITO grain size was nearly the same for the two substrates. Therefore, we speculate that the larger resistivity is caused by differences in the surface state of the substrates, such as the hardness, orientation, or lattice constant. However, the cause for the difference in resistivity remains unknown.

Fig. 6 shows XRD patterns for the films deposited on glass substrates at various substrate temperatures. The FWHM of the diffraction peaks did not vary with the substrate temperature, while the orientation of the ITO grains in the film did. The resistivity for the polycrystalline film consists of both the grain boundary resistance between adjacent ITO grains and that of the ITO grains. The number of grain boundaries through which the current flows is inversely proportional to the particle size. Since the crystal structure of ITO is cubic, the contribution of the ITO grains to the resistivity is independent of their orientation. In contrast, the contribution of grain boundaries to the resistivity does depend on the orientation. Therefore, we speculate that, in the case of ITO thin films, the grain boundary resistance is much larger than that of the ITO grains.

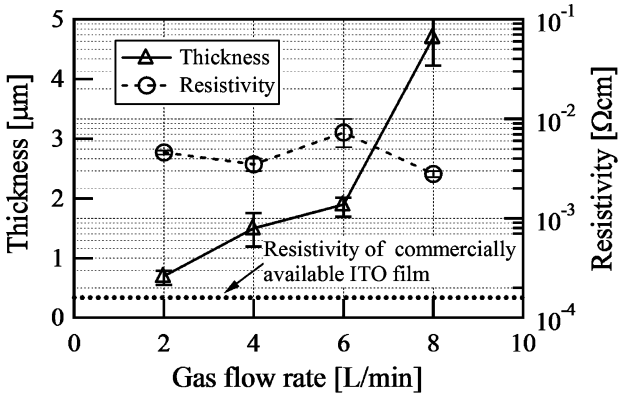

Fig. 4: Dependence of both the film thickness and the resistivity on the gas flow rate at room temperature.

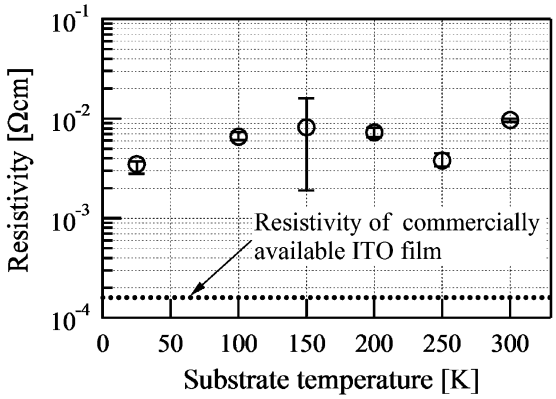

Fig. 5: Dependence of resistivity on substrate temperature.

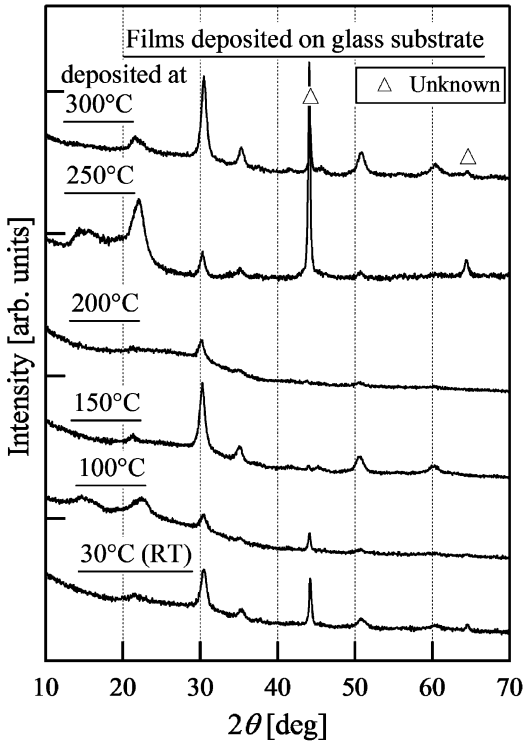

Fig. 6: XRD patterns of films deposited on glass substrates at various substrate temperatures.

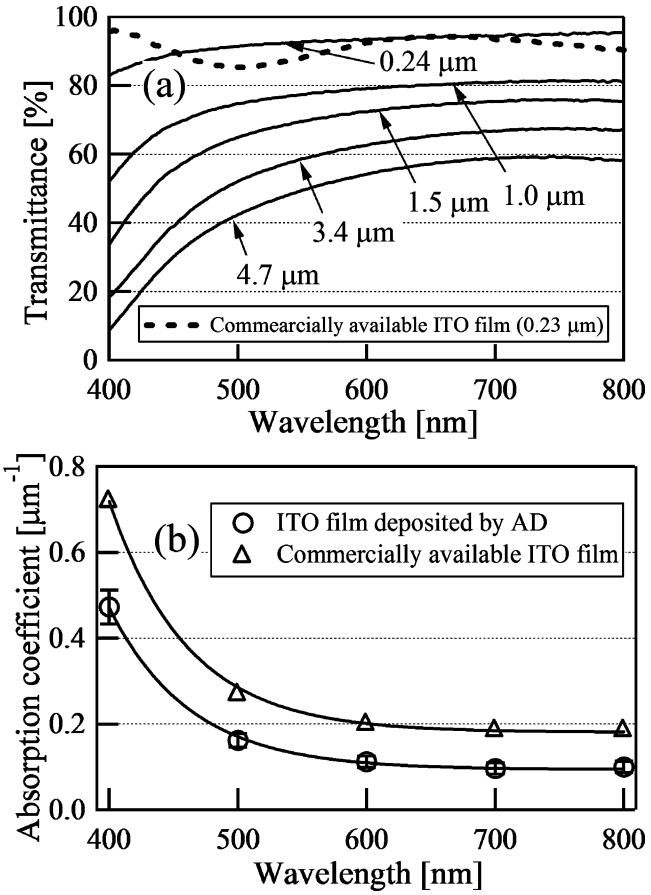

Fig. 7: Wavelength dependences of optical transmittance (a) and the absorption coefficients (b) for ITO films deposited on glass substrate.

Fig. 7(a) shows the wavelength dependence of the optical transmittance for the ITO thin films deposited on the glass substrates. The transmittance of the ITO thin film with a thickness of 4.7 μm was between 9 – 59 % in the wavelength range of 400 – 780 nm. The transmittance increased with decreasing film thickness, to 83 – 95 % for the film with a thickness of 0.24 μm. The dashed line shown in Fig. 7(a) shows the transmittance of commercially available ITO thin film. The transmittance of the ITO thin films deposited using AD was the same as or higher than that of the commercially available ITO thin film. According to Lambert's law, the transmittance is given by

$$Transmittance = \exp(-\alpha d) \quad (1)$$

where α is the absorption coefficient and d is the film thickness. Fig. 7(b) shows the relation between the absorption coefficient and wavelength λ

$$a = A\exp(-\beta\lambda) \quad (2)$$

where A and β are constants. The absorption coefficient of the ITO thin film depends on the wavelength and exponentially decreases with increasing wavelength. The absorption coefficient for the ITO thin films deposited by AD was approximately 40 % smaller than that for commercially available ITO thin film, which means that the transmittance of the ITO thin film deposited by AD was higher. This is because the Rayleigh scattering coefficient in the visible light region for AD-deposited ITO thin film is small, due to the pulverization of the source ITO particles to several tens of nm.

IV. Summary

ITO thin films were formed on glass and sapphire substrates by means of aerosol deposition (AD), and were found to maintain the same crystal structure as the source ITO particles. The resistivity of the film deposited on glass was approximately 3.0×10^{-3} Ω·cm. When the film thickness was 0.24 μm, the film exhibited a high optical transmittance of approximately 90 % in the visible light region. This study demonstrates that, using AD, it is possible to fabricate ITO films with high optical transmittance.

References

1 Nirmal Peiris, T.A., Ghanizadeh, S., Jayathilake, D.S.Y., Hutt, D.A., Wijayantha K.G.U., Conway, P.P., Southee, D.J., Parkin, I.P., Marchand, P., Darr, J.A., Carmalt, C.J.: Aerosol-assisted fabrication of tin-doped indium oxide ceramic thin films from nanoparticle suspensions, *J. Mater. Chem. C*, **4**, 5739 – 5746, (2016).

2 Akedo, J., Ichiki, M., Kikuchi, K., Maeda, R.: Fabrication of three-dimensional microstructure composed of different materials using excimer laser ablation and jet molding, In: IEEE Proc. of MEMS 135 – 140, (1997).

3 Akedo, J., Lebedev, M.: Ceramics coating technology based on impact adhesion phenomenon with ultrafine particles aerosol deposition method for high speed coating at low temperature, *Materia Japan*, **41**, 459 – 466, (2002).

4 Akedo, J., Lebedev, M.: Microstructure and electrical properties of lead zirconate titanate ($Pb(Zr_{52}/Ti_{48})O_3$) thick films deposited by aerosol deposition method, *Jpn. J. Appl. Phys.*, **38**, 5397 – 5401, (1999).

5 Yuki, K., Uemichi, Y., Sato, Y., Yoshikado, S.: Fabrication of nanoporous titanium dioxide films using aerosol deposition, *Key Eng. Mater.*, **566**, 195 – 198, (2013).

6 Akedo, J., Lebedev, M., Iwata, A., Ogiso, H., Nakano, S.: Aerosol deposition method (ADM) for nano-crystal ceramics coating without firing, *MRS Proceedings*, **778**, U8.10.1/W7.10.3, (2003).

7 Lebedev, M., Akedo, J., Ito, T.: Substrate heating effects on hardness of an α-Al_2O_3 thick film formed by aerosol deposition method, *J. Cryst. Growth*, **275**, 1301 – 1306, (2005).

8 Brankovi, Z., Brankovi, G., Tuci, A., Radojkovic, A., Longo, E., Varela, J.A.: Aerosol deposition of $Ba_{0.8}Sr_{0.2}TiO_3$ thin films, *Sci. Sinter.*, **41**, 303 – 308, (2009).

9 Sweet, M.L., Pestov, D., Tepper, G.C., McLeskey, J.T., Jr.: Electrospray aerosol deposition of water soluble polymer thin films, *Appl. Surf. Sci.*, **289**, 150 – 154, (2014).

10 Exner, J., Fuierer, P., Moos, R.: Aerosol deposition of (Cu,Ti) substituted bismuth vanadate films, *Thin Solid Films*, **573**, 185 – 190, (2014).

11 Hsiao, C.C., Luo, L.S.: Gas sensors fabricated by aerosol deposition, *Appl. Mech. Mater.*, **541 – 542**, 151 – 154, (2014).

12 Cullity, B.D., Stock, S.R: Elements of x-ray diffraction, 3rd Ed., Prentice-Hall Inc., pp. 167 – 171, (2001).